

Application of Spray Pyrolysis Process for the Preparation of Nano Sized Cobalt Oxide Powder

Dong Hee Kim¹, Dong Jun Seo² and Jae Keun Yu^{2†}

¹Department of Anesthesiology, Dankook University, Cheonan 330-714, Korea

²Department of Advanced Materials Engineering, Hoseo University, Asan 336-795, Korea

(Received December 1, 2013 : Received in revised form December 10, 2013 : Accepted December 10, 2013)

Abstract In this study, nano-sized cobalt oxide powder with an average particle size below 50 nm was prepared from a cobalt chloride solution by the spray pyrolysis process. The influences of reaction temperature on the properties of the generated powder were examined. The average particle size of the particles formed based on the spray pyrolysis process at a reaction temperature of 700 °C is roughly 20 nm. Moreover, most of these particles cannot appear with an independent type, thereby coexisting in a droplet type. When the reaction temperature increases to 800 °C, the average particle size not only increases to roughly 40 nm but also shows a more dense structure while the ratio of particles which shows a polygonal form significantly increases. As the reaction temperature increases to 900 °C, the distribution of the particles is from roughly 70 nm to 100 nm, while most of the particle surface is more intricately close and forms a polygonal shape. When the reaction temperature increases to 1000 °C, the particle size distribution of the powder shows an existing form from 80 nm to at least 150 nm in an uneven form. As the reaction temperature increases, the XRD peak intensity gradually increases, yet the specific surface area gradually decreases.

Key words nano-sized cobalt oxide powder, cobalt chloride solution, spray pyrolysis process, average particle size, reaction temperature.

1. Introduction

In general, methods of producing minute metallic oxide can largely be classified into the following methods: dry processing method(solid state reaction method),¹⁾ wet process method²⁾ and spray pyrolysis method.³⁻¹⁰⁾ In order to produce high quality functional powder, in general the component ingredients are evenly mixed in a solution to produce a complex acid solution, followed by solidating the acid solution in a reactor referred to as the spray pyrolysis method which is known to be significantly effective. This method not only eliminates the process of mixing solid powder, performing the reaction based on calcination, and grinding to produce powder, but also has the advantage in that the particle characteristics can be controlled based on the pyrolysis conditions and contains little possibility of mixing with impurities. Furthermore, because it is more feasible to eliminate impurities at a solution state rather than a solid state, the aforementioned

method is an appropriate and fair method in producing high purity ingredient powder. Accordingly, Japan's Scimarec, Germany's Merck, and the US's SSC etc all sell high quality ceramic powder based on the spray pyrolysis method. Furthermore, recently studies on producing metallic oxide of nano size based on the spray pyrolysis method is currently being pursued further by Yu,³⁻⁷⁾ Majumdar,⁸⁾ Pluym,⁹⁾ and Messing¹⁰⁾ etc and its application range is significantly expanding. For examples, in steelmakings, spray pyrolysis process is used to manufacture iron oxide powder from the waste acid solution produced in the process of rinsing the surface of hot rolled steel sheets with hydrochloric acid solution. Also, tin oxide powder with an average particle size below 50 nm is manufactured from tin chloride solution,³⁾ and nickel oxide powder with an average particle size of under 50 nm is manufactured from nickel chloride solution.⁴⁾ However, the spray pyrolysis method hasn't been applied for the manufactures of nano-sized cobalt oxide powder; its

[†]Corresponding author

E-Mail : jkyou@hoseo.edu (J. K. Yu, Hoseo Univ.)

© Materials Research Society of Korea, All rights reserved.

This is an Open-Access article distributed under the terms of the Creative Commons Attribution Non-Commercial License (<http://creativecommons.org/licenses/by-nc/3.0>) which permits unrestricted non-commercial use, distribution, and reproduction in any medium, provided the original work is properly cited.

applications for the lithium secondary battery cathode, positive and negative pole materials, catalysts, gas sensors and black matrix materials are expanding rapidly.

In this study, cobalt chloride solution is used as the raw material for the spray pyrolysis process. It produces a cobalt oxide powder with an average particle size below 50 nm. This study is also intended for determining the effects of the reaction temperature on the properties of the produced powder.

2. Experimental

This study uses cobalt chloride (CoCl_2) solution consisting of cobalt ingredients existing in secondary ion form to produce cobalt oxide powder of average particle size of 50 nm or less based on the spray pyrolysis method.

$\text{CoCl}_2 \cdot 6\text{H}_2\text{O}$ of purity 99 % is added to water which is created by an ultra-pure production equipment composed of 4 levels to produce cobalt chloride solution, and the concentration of cobalt is adjusted to 100 g/L respectively. This solution is filtered three times through filter paper to be used as a the final solution for the spray pyrolysis reaction. The following components SiO_2 , P, Ca, Cr and Cu of less or equal to 50 ppm are included within the solution.

In order to conduct the study and create cobalt oxide nano powder of average particle size of under 50 nm through the spray pyrolysis process using the cobalt chloride solution produced, a relevant spray pyrolysis equipment is personally designed and produced for the study. In other words, a spray pyrolysis system is created which could efficiently atomize the solution, spray the solution within the reactor, produce an even heat distribution within the reactor, perfectly proceed the spray pyrolysis reaction, efficiently collect the formed powder inside a bag filter collecting equipment, and include scrubber equipment which can clean harmful gases created. The schematic diagram of this system is shown in Fig. 1. A titanium nozzle is used as the atomizer for

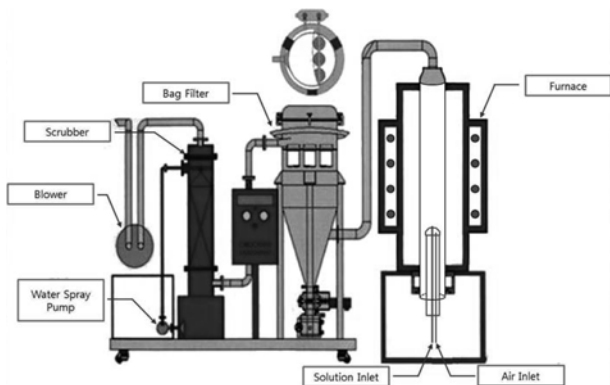


Fig. 1. Schematic diagram of spray pyrolysis system.

the solution.

This study inserts the component solution within the reactor which is maintained at a temperature of 700~1000 °C through a nozzle and sprayed in an atomized droplet form to produce powder of average particle size equal to or less than 50 nm. The component solution is inserted into one entrance of the nozzle at a velocity of 10 ml/min through a quantitative chemical pump while air compressed through an air compressor at a pressure of 3 kg/cm² is inserted into the other entrance of the nozzle to atomize the solution. Given reaction conditions, the properties of the correspondingly produced powder are examined by TEM (JEM-2100F, JEOL Ltd.) analysis (whether the production of single crystal particles), SEM (Quanta 200, FEI Ltd.) analysis (particle size distribution and particle shape), XRD (D/Max-2500V, Rigaku Ltd.) analysis (powder phase and composition), and the measurement of specific surface area (ASAP 2020, micromeritics Ltd.).

3. Result and Discussion

3.1 Thermodynamic considerations for spray pyrolysis process

When the cobalt component presents with divalent ions in raw material solution, thermodynamic pyrolysis reactions for the production of solid cobalt oxide can be expressed through the following reactions.¹¹⁾

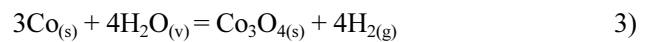


$$\Delta G^\circ = -884,916 + 360.24 T \text{ Joules} \quad (1-1)$$



$$\Delta G^\circ = -246,438 + 54.81 T \text{ Joules} \quad (2-1)$$

Multiplying equation 2) by 4 and deducting equation 1) derives at equation 3).



$$\Delta G^\circ = 100,836 + 141 T \text{ Joules} \quad (3-1)$$

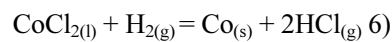


$$\Delta G^\circ = -188,200 - 12.8 T \text{ Joules} \quad (4-1)$$



$$\Delta G^\circ = -302,085 - 16.7 T \ln T + 228.1 T \text{ Joules} \quad (5-1)$$

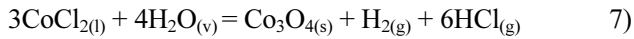
Deducting equation 5) from equation 4) derives at equation 6).



$$\Delta G^\circ = 113,885 + 16.7 T \ln T - 240.9 T \text{ Joules} \quad (6-1)$$

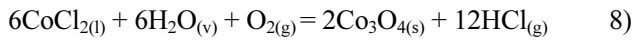
The sum of multiplying equation 6-1), equation 3), and

equation 6) by 3 derives at equation 7).



$$\Delta G^\circ = 442.491 + 50.1 T \ln T - 581.7 T \quad 7-1)$$

The sum of multiplying equation 2) by 2 and multiplying equation 7) by 2 derives at the study's pyrolysis reaction formula of equation 8).



$$\Delta G^\circ = 389,982 - 1,051.7 T + 100.2 T \ln T \text{ Joules} \quad 8-1)$$

Accordingly, value of the changes in the standard free energy at the reaction temperatures regarding equation 8) of 700 °C, 800 °C, 900 °C and 1000 °C respectively are 37,478, 11,768, -13,007 and -36,927 J.

However, whether Co_3O_4 is formed in solid state based on the pyrolysis reaction is not based on ΔG° as reflects per equation 8-1) but can be reflects as ΔG as per equation 8-2).

$$\Delta G = \Delta G^\circ + RT \ln(a_{\text{Co}_3\text{O}_4}^2 \cdot P_{\text{HCl}}^{12} / a_{\text{CoCl}_2}^6 \cdot P_{\text{H}_2\text{O}}^6 \cdot P_{\text{O}_2}) \quad 8-2)$$

In this regards, ΔG reflects the changes in free energy based on random conditions, while ΔG° , a and P reflects the changes in standard free energy, activity and partial pressure respectively.

Results of this study reflects the formation of cobalt oxide (Co_3O_4) in solid form even in a reaction temperature of 700 °C. Despite the ΔG° 's plus (+) value in equation 8-2), this result shows that the absolute value of $RT \ln(a_{\text{Co}_3\text{O}_4}^2 \cdot P_{\text{HCl}}^{12} / a_{\text{CoCl}_2}^6 \cdot P_{\text{H}_2\text{O}}^6 \cdot P_{\text{O}_2})$ reflects a greater minus (-) value, thereby resulting in an overall negative (-) value in the ΔG value.

3.2 Effects of the reaction temperature on the properties of produced powder

The characteristic changes of the particles magnified by 5,000 times based on the SEM is shown in Fig. 2 when the reaction temperature is adjusted from 700 °C to 1,000 °C given the following conditions: the Co ingredient within the solution is set at 100 g/L, the inflow speed of the solution at 10 ml/min, nozzle tip size at 2 mm, and air pressure at 3 kg/cm².

Because the solution is atomized by the nozzle to form

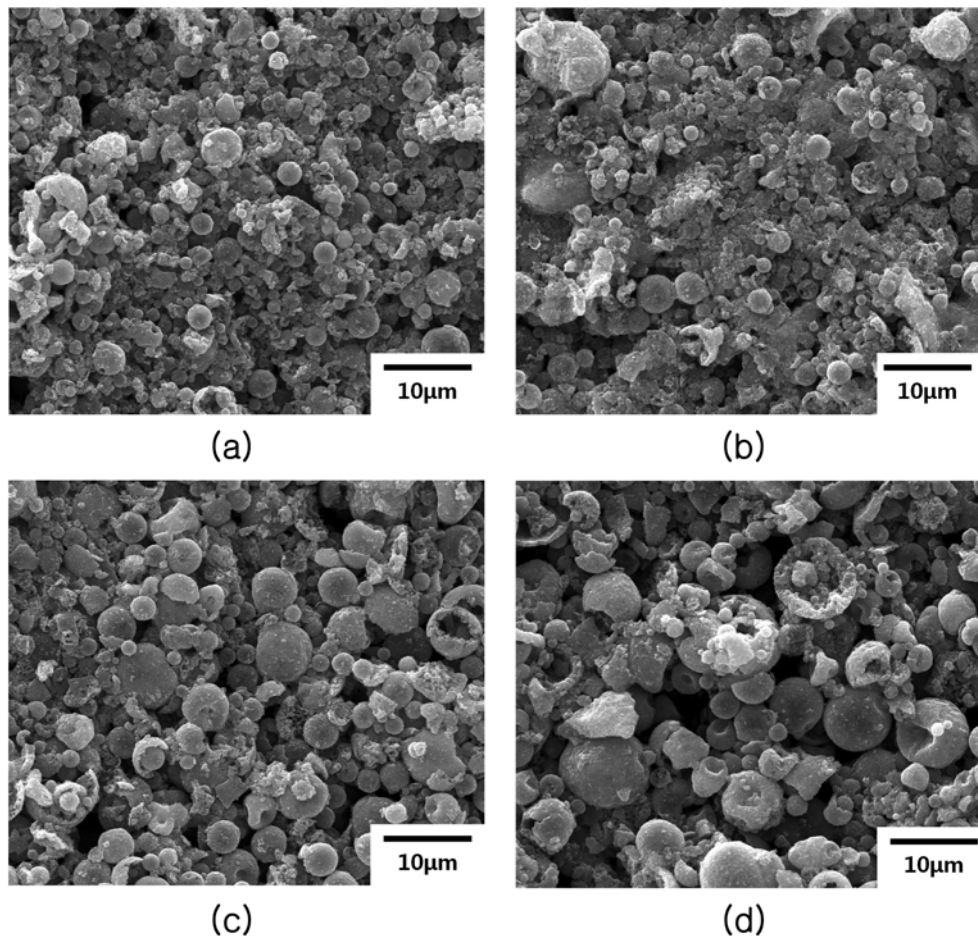


Fig. 2. SEM photographs of produced powder according to reaction temperature at raw material solution of 100 g/l Co, 10 ml/min. inflow speed of the solution, 2 mm nozzle tip size and 3 kg/cm² air pressure (× 5,000). (a) 700 °C, (b) 800 °C, (c) 900 °C, (d) 1,000 °C.

a droplet and is flowed into the reactor to perform the pyrolysis reaction, the CoCl_2 solute solidifies from the droplet surface to be extracted. As a result, if the solvent existing inside the droplet fails to smoothly pass through the upper level of the surface, the pressure inside the droplet increases and ultimately the droplet starts to divide. When the droplet atomized at a reaction temperature of 700°C flows into the reaction domain, the solvent begins to evaporate in the surface. However, due to the relatively low concentration of Cobalt within the solution at 100 g/L and relatively low reaction temperature, there is relatively insignificant concentration difference between i) the surface of the droplet until the solvent becomes completely evaporated within the droplet; and ii) the central area. Accordingly, a severe droplet division does not occur during the pyrolysis process. As the results show as per Fig. 2(a), the powder formed based on the pyrolysis reaction reflects a higher ratio of initial circular atomized droplet form compared to other reaction temperatures. Alternatively, results shows that when the reaction temperature is increases to 800°C , the ratio of droplet form which reflects cohesion amongst the minute

powder decreases while the droplets divided more severely. As reflects per the results in the reaction formula 1), the size of the initial droplet which is atomized by the nozzle is irrelevant to the reaction temperature, however, it is assumed that the increase in reaction temperature during the pyrolysis reaction process resulted in a more severe droplet division.

$$X = 585 \frac{\sqrt{\sigma}}{\nu \sqrt{\sigma}} + 579 \left(\frac{\mu}{\nu \sqrt{\sigma \rho}} \right)^{0.45} \frac{1000 Q_L}{Q_a}^{1.5} \quad (9)$$

In the formula above, X reflects the average particle size, σ reflects the surface tension of the solution, ρ reflects the density, ν reflects the spray speed of the solution, μ reflects the viscosity, Q_L reflects the amount of the solution, and Q_a reflects the amount of air inflow.

Alternatively, when the reaction temperature is set at 800°C , the ratio of the droplets in circular shape rather decreases compared to other higher reaction temperatures. This result is assumed to be due to the following reason: following the division of the droplets, it is assumed that the temperature of 800°C seems to be

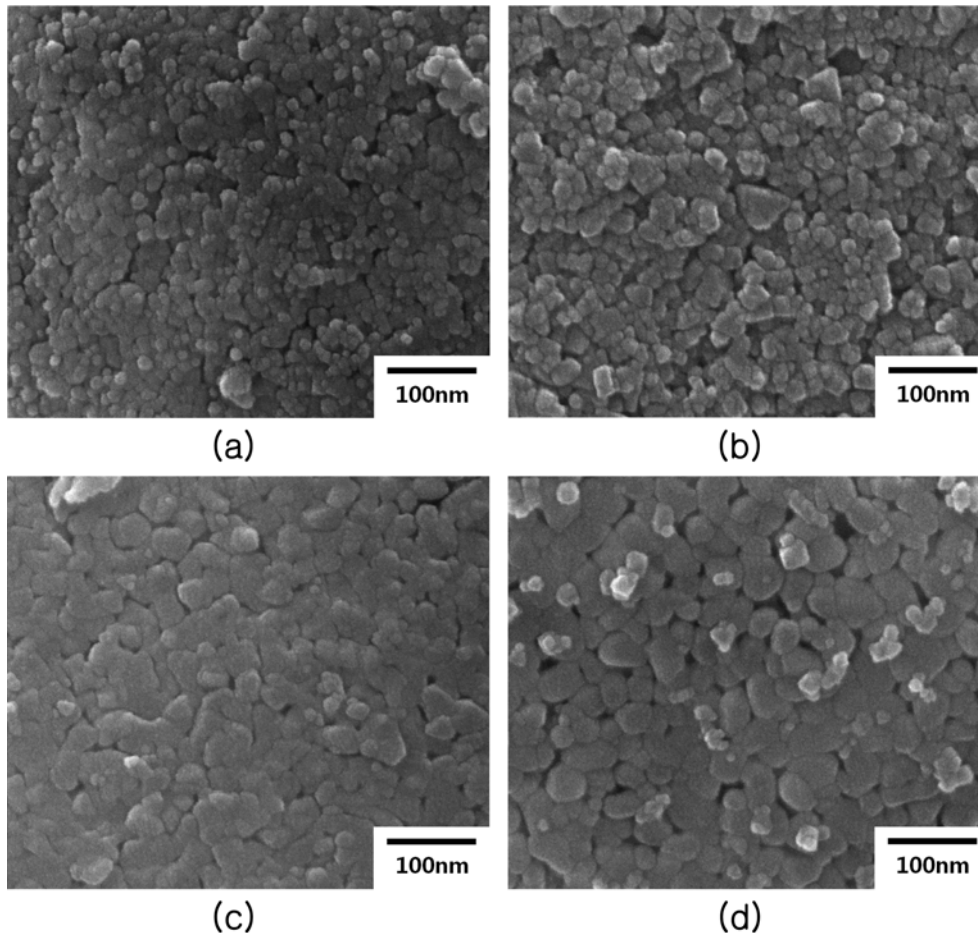


Fig. 3. SEM photographs of produced powder according to reaction temperature at raw material solution of 100 g/l Co, 10 ml/min . inflow speed of the solution, 2 mm nozzle tip size and 3 kg/cm^2 air pressure ($\times 300,000$). (a) 700°C , (b) 800°C , (c) 900°C , (d) $1,000^\circ\text{C}$.

insufficient to re-combine the divided droplets. When the reaction temperature is set at 900 °C, whereas the droplet division occurs relatively more severely during the pyrolysis process, the droplets which are divided at the high temperatures start to combine, thereby re-increasing the ratio of droplets in circular form. Alternatively, reaction temperature set at 1000 °C reflects a very severe droplet division, resulting in an extremely uneven distribution of the droplet size. Furthermore, the combination which occurs between or inside the droplets due to the high temperature resulted in a very elaborate surface structure.

The results of characteristic changes of the particles magnified by 300,000 times based on the SEM given the same reaction conditions as in Fig. 2 is shown in Fig. 3. Results of Fig. 3(a) show that the average particle size of the droplet form reflects in Fig. 2(a) is roughly 20 nm, composed of nano particles. This result is assumed to be due to the following reason: Because the droplet division does not occur severely, most of the final particles formed based on the pyrolysis reaction failed to show an inde-

pendent form and coexisted within the initial atomized droplet. Furthermore, the relatively low reaction temperature seems to have led to an insufficient sintering reaction, thereby forming extremely minute particles of average particle size at 20 nm. When the reaction temperature is set at 800 °C, the even quicker evaporation of the solvent within the solution due to the temperature increase leads to supersaturation of the solvent in the droplet surface. Furthermore, because the droplet division occurs more severely in the initial stages of the pyrolysis process, the particle size distribution of the powder formed is more uneven compared to when the reaction temperature is 700 °C. Alternatively, the sintering process of the ultra-fine particles initially formed based on the pyrolysis reaction at high reaction temperatures proceeds faster, resulting in an average particle size of 30 nm. This result reflects not only an increase compared to when the reaction temperature is set at 700 °C, but also a more close structure, thereby showing that the ratio of the particles of polygonal form had significantly increased. When the reaction temperature

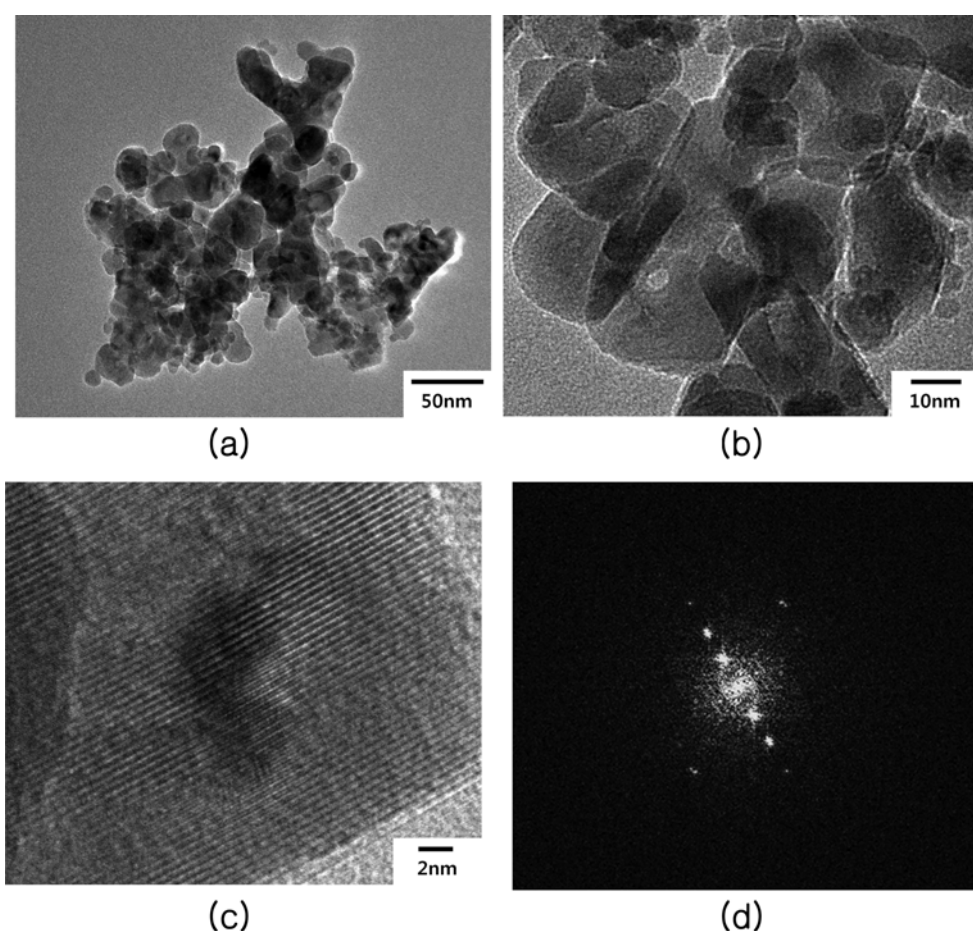


Fig. 4. TEM photographs of produced powder and selective diffraction pattern of single particle at reaction temperature of 800 °C, raw material solution of 100 g/L Co, 10 ml/min. inflow speed of the solution, 2 mm nozzle tip size and 3 kg/cm² air pressure. (a) TEM photographs of produced powder($\times 300,000$), (b) TEM photographs of produced powder($\times 1,000,000$), (c) HRTEM image of an individual Co₃O₄ nanocrystal, (d) Selective diffraction pattern of single particle.

is set at 900 °C, the significantly high reaction temperature leads to a instant solidification of the droplet surface, thereby significantly increasing the pressure inside the droplet and resulting an even more severe division of the droplets at the initial stages of the pyrolysis reaction. Accordingly, although the particle size of the solid powder formed at the initial stage of the reaction are very small, because the sintering process proceeds very quickly due to the high reaction temperature, the particle size distribution of the final powder formed exists from roughly 70 nm to at least 100 nm. Overall, the average particle size of the powder significantly increases compared to when the reaction temperature is 800 °C. Not only is the particle surface intricately close but also most of the particles developed reflects a polygonal form in near circular form. Alternatively, when the reaction temperature is set at 1000 °C, severe division of the droplets occur at the initial stage of the reaction due to the instant oversaturation of the droplet surface and the significant increase of the internal pressure within the droplet. Accordingly, although the particle size of the solid powder formed at the initial reaction stage is very small, because the sintering process proceeds extremely quickly due to the high reaction temperature, the particle distribution of the final powder formed ranged from 80 nm to at least 150 nm, reflecting a very uneven form. Alternatively, the overall average particle size of the powder significantly increases compared to when the reaction temperature is 900 °C. And, not only is the particle surface intricately close but also the sintering process is considered as an significant progress.

The structural characteristics of the particles formed based on the pyrolysis process using TEM is shown in Fig. 4. The states of the particles expanded by 300,000 times, 1,000,000 times, and 4,000,000 times are shown in Fig. 4(a), (b) and (c), and assesses whether single crystals are formed at the primary level. Furthermore, the diffraction pattern of a random particles is shown in Fig. 4(d). Other particles also shows nearly the same pattern and these results concluded that the particles formed an intricately close single crystal structure.

The results of XRD analysis under the same reaction conditions as in Fig. 2 is shown in Fig. 5 as the reaction temperature increase from 700 °C to 1,000 °C, and shows the corresponding Miller Index of each peak. Irrelevant to the reaction temperature, only the phase of Co_3O_4 exists. Furthermore, when the reaction temperature is set at 700 °C, the Miller index relevant to the primary, secondary and tertiary peak is (311), (440) and (220) respectively. Alternatively, when the reaction temperature is set at 800 °C or above, the Miller index related to the primary, secondary, and tertiary peak is (311), (220), and (440) respectively. Even at the lowest reaction temperature of 700 °C, unreactive products of Cobalt chloride (CoCl_2)

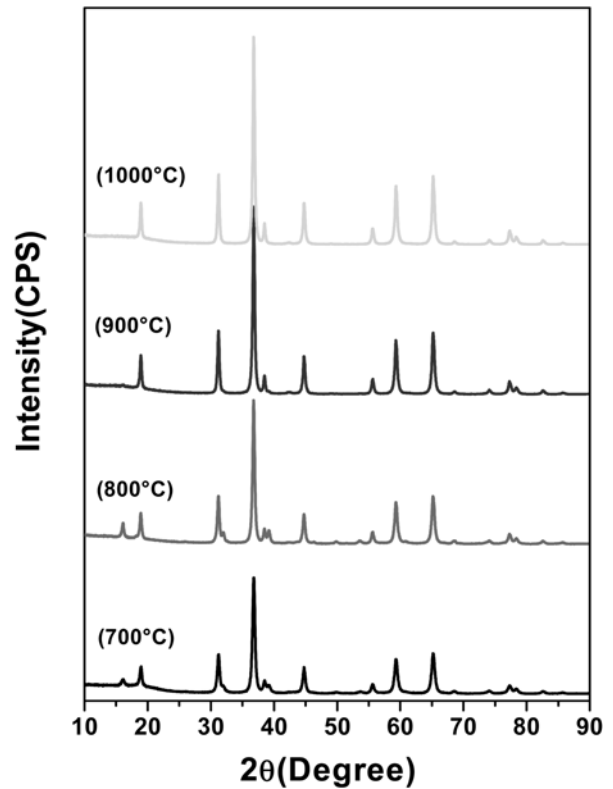
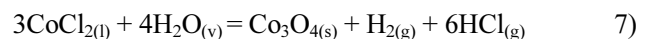


Fig. 5. XRD patterns of powder according to reaction temperature at raw material solution of 100 g/l Co, 10 ml/min. inflow speed of the solution, 2 mm nozzle tip size and 3 kg/cm² air pressure. (a) 700 °C, (b) 800 °C, (c) 900 °C, (d) 1,000 °C.

did not occur, and this result concluded that sufficient pyrolysis reaction as reflects per equation (7) had proceeded despite the short reaction time period within the reaction temperature range.



As the reaction temperature increases from 700 °C to 1,000 °C, the strength of the diffraction peak related to each Miller index reflects a gradual increase. This result is assumed to be based on the following reason: as the reaction temperature increases from 700 °C to 800 °C, the average particle size of the particles formed based on the pyrolysis reaction significantly increased, ranging from roughly 20 nm to 30 nm while the ratio of particles reflecting a more intricately close polygonal form significantly increased. Additionally, when the reaction temperature increases to 900 °C, the particle distribution of the particles formed existed from roughly 70 nm to at least 100 nm. Overall, the average particle size of the powder significantly increases compared to when the reaction temperature is set at 800 °C while the most of the particle surface is more intricately close and formed a polygonal form in near circular form. This is assumed to

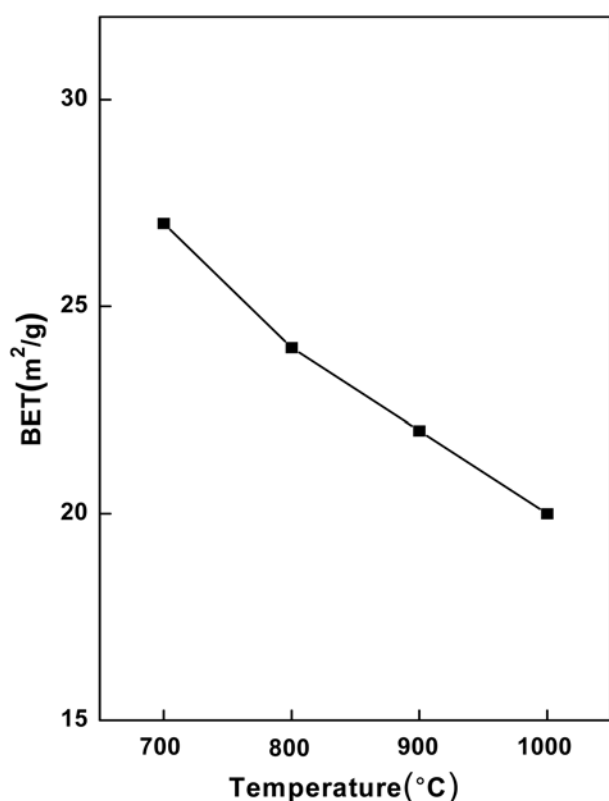


Fig. 6. Specific surface areas of powder according to reaction temperature at raw material solution of 100 g/l Co, 10 ml/min. inflow speed of the solution, 2 mm nozzle tip size and 3 kg/cm² air pressure.

have significantly increases the strength of the peaks. On the other hand, when the reaction temperature is set at 1000 °C, the particle distribution of the powder formed existed in the range of 100 nm to at least 150 nm due to the higher reaction temperature, thereby overall significantly increasing the average particle size of the powder compared to when the reaction temperature is 900 °C. Furthermore, not only is the particle surface more intricately close but also the sintering process reflects a significantly progress. This is assumed to have significantly increases the strength of the XRD peaks.

The changes in the specific surface area of the powder formed following changes in the reaction temperature is shown in Fig. 6. As the reaction temperature increases from 700 °C to 1,000 °C, the specific surface area gradually decreased, however, in comparison to the increase in the average particle size of the particles as shown in Fig. 3, the decrease in the specific surface area is not significant. This result is assumed to be based on the following reason: the decrease effect of specific surface area due to an increase in the average particle size of the particles by the increase in reaction temperature is partly canceled by the increase effect of specific surface area due to a droplet type spilted more significantly as shown in Fig. 2 as the reaction temperature increases. As the

reaction temperature increases from 700 °C to 800 °C, the specific surface area decreases by roughly 10 %. This results is assumed to be based on the following reason: as shown in Fig. 3(a) and (b), as the reaction temperature increases from 700 °C to 800 °C, the average particle size of the particles significantly increases from 20 nm to at least 30 nm, leading to a significant decreasing effect in the specific surface area. However, this decreasing effect seems to be partially offset by the increasing effects of the specific surface area resulting from the decrease in the ratio of spherical droplet form and severely spilted form following an increase in the reaction temperature as shown in Fig. 2(a) and (b). When the reaction temperature is increases to 900 °C and 1,000 °C, the specific surface area decreases by roughly 10 % respectively. In other words, as shown in Fig. 3(c) and (d), the average particle size of the particles significantly increases to 70 nm and at least 100 nm respectively, however, the specific surface area decreases relatively little in comparison. This result is assumed to be based on the following reason: as shown in Fig. 3(c) and (d), the increasing effects of the specific surface area due to the significant increase in the ratio of severely divided droplet form following an increase in the reaction temperature seems to offset the decreasing effects in the specific surface area due to the increase in the average particle size of the particles following an increase in the reaction temperature.

4. Conclusions

This study has produced cobalt oxide powder of average particle size equal to or under 50 nm based on the spray pyrolysis reaction using a self made spray pyrolysis equipment using cobalt chloride solution and has assessed the characteristic changes of the particles following changes in reaction temperature and concentration of the solution.

When the reaction temperature is set at 700 °C, the insufficient sintering process resulted in an average particle size of the particles formed based on the reaction at roughly 20 nm and most of these particles failed to form an independent form within the droplet. When the reaction temperature is 800 °C, the higher reaction temperature resulted in a quicker sintering process of the initially formed ultra-fine particles based on the pyrolysis reaction, thereby increasing the average particle size at roughly 40 nm, reflecting a more intricately close structure, and significantly increasing the ratio of particles in polygonal form. When the reaction temperature is 900 °C, the droplet division occurred very severely, however due to the quick sintering process under the high reaction temperature, the particle distribution of the final powder formed ranged from roughly 70 nm to at least 100 nm.

When the reaction temperature is set at 1000 °C, the particle distribution of the final powder formed ranged from 80 nm to at least 150 nm in a very uneven form. XRD analysis shows that as the reaction temperature increases from 700 °C to 1,000 °C, the intensity of the diffraction peaks shows a gradual increase. Alternatively, when the reaction temperature increases from 700 °C to 1,000 °C, the specific surface area reflects a gradual decrease.

References

1. T. Nakamura and Y. Okano, *Proceeding of the ICF* **7**, C1-101 (1996).
2. C. P. Udawatte and K. Yanagisawa, *J. Am. Ceram. Soc.*, **84**(1), 251 (2001).
3. J. K. Yu and D. H. Kim, *Kor. J. Mater. Res.*, **23**(2), 81 (2013)
4. J. K. Yu and D. H. Kim, *Powder Tech.*, **235**(2), 1030 (2013)
5. J. K. Yu and D. H. Kim, *J. of Nanosci. Nanotechnol.*, **12**(2), 1545 (2012)
6. J. K. Yu and D. H. Kim, *J. Ceram. Soc. Jpn.*, **117**(10), 1078 (2009).
7. J. K. Yu, S. G. Kang, K. C. Chung, J. S. Han and D. H. Kim, *Mater. Trans.*, **48**(2), 249 (2007).
8. J. K. Yu, S. G. Kang, J. B. Kim, J. Y. Kim, J. S. Han, J. W. Yoo, S. W. Lee and Z. S. Ahn, *Mater. Trans.*, **47**(7), 1838 (2006).
9. J. K. Yu, K. W. Kim, T. S. Kim and J. Y. Kim, *Mater. Trans.*, **46**(7), 1695 (2005).
8. D. Majumdar, T. A. Shefelbine and T. T. Kodas, *J. Mater. Res.*, **11**(11), 2861 (1996).
9. T. C. Pluym and T. T. Kodas, *J. Mater. Res.*, **10**(7), 1661 (1995).
10. G. L. Messing, S. C. Zhang and G. V. Jayanthi, *J. Am. Ceram. Soc.*, **76**(11), 2707 (1993).
11. I. Barin: *Thermochemical Data of Pure Substances*, VCH, Germany, 1392-1404 (1989).